Mathematical Medicine and Biology: A Journal of the IMA (2026) **00**, 1–15
https://doi.org/TBD

Warped-Seam Geometry and Canalization as Gromov–Hausdorff Collapse

LARS RÖNNBÄCK*
Department of Computer and Systems Sciences, Stockholm University, Stockholm, Sweden
*Corresponding author: lars@uptochange.com

[Received on Date Month Year; revised on Date Month Year; accepted on Date Month Year]

Waddington's epigenetic landscape is often drawn as a "ball rolling" picture; here we give a concrete metric realization directly on gene-expression space $\mathbb{R}^n$. Given a smooth nonnegative scalar field s ("landscape height") and an admissible warping function ϕ with $\phi(0) = 0$, we deform the Euclidean metric conformally by the factor $\phi(s)^2$. The resulting length metric collapses distances inside each basin of attraction. Under Morse, separation, and properness assumptions on s, we prove that the compact sublevel sets $X_\varepsilon = \{s \le \varepsilon\}$ converge in the Gromov–Hausdorff sense to a finite discrete metric space with one point per global minimum, and establish a sharp two-sided bound $\operatorname{diam}(X_\varepsilon^{(i)}, d_\phi) = \Theta(\varepsilon^{\alpha+1/2})$ for power-law warping $\phi(s) = s^\alpha$. We extend the framework to Morse–Bott landscapes, where the zero set of s is a union of compact connected submanifolds—modelling attracting cell-type manifolds rather than isolated fixed points—and show that each connected component still collapses to a single point under d_ϕ. We connect the warped metric to the Freidlin–Wentzell quasi-potential for the gradient stochastic differential equation $\mathrm{d}X = -\nabla s(X)\,\mathrm{d}t + \sqrt{2T}\,\mathrm{d}W$, showing that the quasi-potential is itself a warped length metric with position-dependent weight $|\nabla s|$, and that the dynamically natural choice $\phi(s) = \sqrt{s}$ arises from the local quadratic structure of s near its minima. Finally, we illustrate the theory on a two-dimensional toggle-switch landscape modelling mutual gene repression, computing collapse rates and inter-basin distances explicitly.

Keywords: canalization; Waddington landscape; Gromov–Hausdorff convergence; Morse theory; Freidlin–Wentzell theory.

1. Introduction and Overview

In developmental biology, *canalization* refers informally to robustness: many nearby states lead to the same outcome. Waddington's epigenetic landscape (Waddington, 1957) depicts this as valleys separated by ridges, and a large body of quantitative work—from quasi-potential reconstructions in gene-regulatory networks (Wang et al., 2011; Zhou et al., 2012) to single-cell trajectory inference (Rizvi et al., 2017; Schiebinger et al., 2019)—has sought to make this picture precise.

This paper isolates a minimal geometric statement capturing one aspect of that picture: as we restrict to low landscape height $s \le \varepsilon$, each basin becomes metrically small, while distinct basins remain at a finite distance from each other. The mechanism is simple: define a weighted length functional where the cost of motion is multiplied by a factor $\phi(s)$ that vanishes at the global minima of s. Inside a low sublevel set, motion can "hug" the minimum and become cheap; any path connecting distinct minima must cross a ridge where s is bounded away from 0, forcing positive length.

We call the resulting structure a *warped-seam geometry*: the *seam* is the scalar field s itself—so named because it encodes how the space is stitched together, prescribing where basins meet and where ridges separate them. The *warping* is the rule ϕ that converts the seam into a genuine metric via $g_\phi = \phi(s)^2 g_F$. Together, the seam tells us *what* the geometric structure is; the warping tells us *how strongly* it is felt (see Figure 1).

Gromov–Hausdorff convergence of degenerating metric spaces is a well-developed subject. The Cheeger–Gromov–Fukaya theory (Cheeger and Gromov, 1986; Fukaya, 1987) studies collapsing of Riemannian manifolds under curvature bounds—a substantially deeper phenomenon than what occurs here. Our collapsing mechanism is more elementary: the conformal factor $\phi(s)$ simply vanishes at the minima, making basins metrically small without any curvature control. Our contribution is not the collapsing mechanism itself but its application to the canalization setting: we identify the biologically meaningful assumptions under which GH collapse occurs, establish sharp rates, connect the warped metric to stochastic dynamics, and provide explicit computations for gene-regulatory models.

Contributions. Beyond the basic Gromov–Hausdorff collapse theorem (Theorem 6.2), we make four additional contributions:

(1) *Sharp collapse rate* (Proposition 7.2). We prove a matching lower bound on the diameter, yielding $\operatorname{diam}(X_\varepsilon^{(i)}, d_\phi) = \Theta(\varepsilon^{\alpha+1/2})$ for $\phi(s) = s^\alpha$.

(2) *Morse–Bott generalization* (Theorem 8.4). When the zero set $\{s = 0\}$ is a disjoint union of compact submanifolds—the biologically relevant case where a cell type is a manifold of expression states—the same GH collapse holds.

(3) *Freidlin–Wentzell connection* (Section 9). We show the quasi-potential of the gradient SDE $\mathrm{d}X = -\nabla s\,\mathrm{d}t + \sqrt{2T}\,\mathrm{d}W$ is itself a warped length metric, and that $\phi(s) = \sqrt{s}$ is the dynamically natural warping.

(4) *Toggle-switch example* (Section 10.2). We work out a concrete two-dimensional bistable landscape modelling mutual gene repression, computing inter-basin distances and collapse rates explicitly.

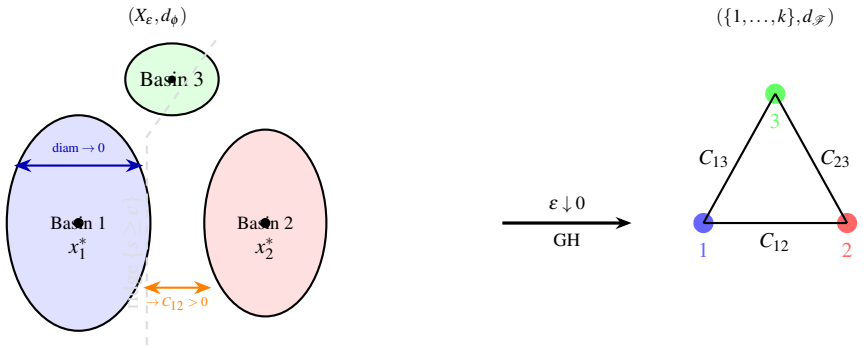

Figure 1. Schematic of Gromov–Hausdorff collapse. Left: the sublevel set X_ε with three basins separated by ridges (dashed). Under the warped metric d_ϕ, each basin has diameter $\to 0$ while inter-basin distances converge to finite constants C_{ij}. Right: the limit discrete metric space.

2. Geometric Framework

Let $F = \mathbb{R}^n$ with Euclidean metric g_F. Let $s : F \to [0,\infty)$ be smooth.

Definition 2.1 (Admissible warping function) *A function $\phi : [0,\infty) \to [0,\infty)$ is* admissible *if:*

(i)ϕ is continuous on $[0,\infty)$ and smooth on $(0,\infty)$,
(ii)ϕ is strictly increasing,
(iii)$\phi(0) = 0$, and
(iv)$\phi(s) > 0$ for $s > 0$.

Definition 2.2 (Conformal length metric) *Define the conformal (possibly degenerate) tensor*

$$g_\phi := \phi(s(x))^2 g_F.$$

The induced length metric is

$$d_\phi(x,y) = \inf_\gamma \int_0^1 \phi(s(\gamma(u)))\,|\gamma'(u)|\,\mathrm{d}u,$$

where the infimum ranges over piecewise C^1 curves $\gamma : [0,1] \to \mathbb{R}^n$ with $\gamma(0) = x$ and $\gamma(1) = y$.

Remark 2.3 (Degeneracy at minima) *Since $\phi(0) = 0$, the tensor g_ϕ degenerates on the zero set $\{s = 0\}$. Nevertheless the definition above yields an extended length metric on $\mathbb{R}^n$. Under the separation assumption below, distinct minima have strictly positive d_ϕ-distance.*

For subsets $A, B \subset \mathbb{R}^n$ we write

$$d_\phi(A,B) := \inf\{d_\phi(a,b) : a \in A,\, b \in B\}.$$

3. Structural Assumptions

We assume:

(A1)s is Morse.
(A2)s has exactly k nondegenerate global minima $x_1^*,\dots,x_k^*$ with $s(x_i^*)=0$.
(A3)(Ridge separation) There exists $c>0$ such that the connected components of $\{s<c\}$ containing distinct minima have disjoint closures.
(A4)(Properness) $s(x)\to\infty$ as $|x|\to\infty$.

Properness implies all sublevel sets are compact. For $\varepsilon>0$ define

$$X_\varepsilon := \{x\in\mathbb{R}^n : s(x)\le\varepsilon\},$$

and for $0<\varepsilon<c$ let $X_\varepsilon^{(i)}$ denote the component containing x_i^*.

4. Local quadratic control and shrinkage

Lemma 4.1 (Two-sided quadratic control near minima) *For each i there exist constants $r_i>0$ and $0<\lambda_i\le\Lambda_i$ such that for all $|x-x_i^*|<r_i$,*

$$\tfrac{\lambda_i}{2}|x-x_i^*|^2 \le s(x) \le \tfrac{\Lambda_i}{2}|x-x_i^*|^2.$$

Proof Since x_i^* is a nondegenerate minimum, $\operatorname{Hess} s(x_i^*)$ is positive definite. By continuity of $\operatorname{Hess} s$ there is a neighborhood where the eigenvalues of $\operatorname{Hess} s(x)$ lie in $[\lambda_i,\Lambda_i]$. Integrating the second-order Taylor formula along the segment from x_i^* to x gives the stated two-sided bounds. □

Lemma 4.2 (Sublevel shrinkage in Euclidean diameter) *For each i there exists $C_i>0$ such that for all sufficiently small ε,*

$$\operatorname{diam}(X_\varepsilon^{(i)}, g_F) \le C_i\sqrt{\varepsilon}.$$

Proof By Lemma 4.1, $s(x)\le\varepsilon$ implies $|x-x_i^*|\le\sqrt{2\varepsilon/\lambda_i}$. Hence $X_\varepsilon^{(i)}$ is contained in a Euclidean ball of that radius, and its Euclidean diameter is $O(\sqrt{\varepsilon})$. □

Lemma 4.3 (Distance to the minimum) *For each i there exist $\varepsilon_i>0$ and $K_i>0$ such that for all $0<\varepsilon\le\varepsilon_i$ and all $x\in X_\varepsilon^{(i)}$,*

$$d_\phi(x,x_i^*) \le K_i\,\phi(\kappa_i\varepsilon)\,\sqrt{\varepsilon},$$

where $\kappa_i:=\Lambda_i/\lambda_i$ comes from Lemma 4.1. Consequently, $\sup_{x\in X_\varepsilon^{(i)}} d_\phi(x,x_i^*)\to 0$ as $\varepsilon\downarrow 0$.

Proof Take ε small enough that $X_\varepsilon^{(i)}\subset B(x_i^*,r_i)$ with r_i from Lemma 4.1. Fix $x\in X_\varepsilon^{(i)}$ and consider the Euclidean segment $\gamma(t)=x_i^*+t(x-x_i^*)$.

For $t \in [0,1]$, Lemma 4.1 gives

$$s(\gamma(t)) \le \tfrac{\Lambda_i}{2} t^2 |x - x_i^*|^2 \le \tfrac{\Lambda_i}{\lambda_i}\,\varepsilon,$$

since $|x - x_i^*|^2 \le 2\varepsilon/\lambda_i$. Thus $\phi(s(\gamma(t))) \le \phi((\Lambda_i/\lambda_i)\varepsilon) = \phi(\kappa_i\varepsilon)$ and

$$d_\phi(x, x_i^*) \le \int_0^1 \phi(s(\gamma(t)))|\gamma'(t)|\,\mathrm{d}t \le \phi(\kappa_i\varepsilon)\,|x - x_i^*|.$$

Using $|x - x_i^*| \le \sqrt{2\varepsilon/\lambda_i}$ yields the bound with a constant K_i. □

Remark 4.4 (When $\phi(\kappa\varepsilon) \asymp \phi(\varepsilon)$) *For common choices such as $\phi(s) = s^\alpha$ (or more generally ϕ regularly varying at 0), one has $\phi(\kappa\varepsilon) \asymp \phi(\varepsilon)$ for each fixed $\kappa > 0$. In that case Lemma 4.3 can be stated with $\phi(\varepsilon)$ up to a change in constants.*

5. Inter-basin distances

Fix $c > 0$ from (A3). For each minimum define the basin at height c:

$$A_i(c) := \text{the connected component of } \{s < c\} \text{ containing } x_i^*.$$

Define the Euclidean gap

$$w_{ij} := \operatorname{dist}_{g_F}(\overline{A_i(c)}, \overline{A_j(c)}).$$

By (A3) and compactness of the closures, $w_{ij} > 0$ for $i \ne j$.

Definition 5.1 (Inter-basin constants) *For $i \ne j$ define*

$$C_{ij} := d_\phi(x_i^*, x_j^*).$$

Lemma 5.2 (Positivity and finiteness) *For $i \ne j$ we have $0 < C_{ij} < \infty$.*

Proof Finiteness follows because $\mathbb{R}^n$ is path connected and $\phi \circ s$ is finite everywhere.

For positivity, any curve from x_i^* to x_j^* must leave $A_i(c)$ and enter $A_j(c)$, hence must intersect the closed set $\{s \ge c\}$. Along the portion of the curve in $\{s \ge c\}$ we have $\phi(s) \ge \phi(c)$. Moreover the curve must cross the Euclidean gap between the disjoint closed sets $\overline{A_i(c)}$ and $\overline{A_j(c)}$, which forces Euclidean arclength at least w_{ij}. Therefore $C_{ij} \ge \phi(c) w_{ij} > 0$. □

Lemma 5.3 (Distance convergence) *For $i \ne j$,*

$$d_\phi(X_\varepsilon^{(i)}, X_\varepsilon^{(j)}) \to C_{ij} \qquad (\varepsilon \downarrow 0).$$

Proof For any $x \in X_\varepsilon^{(i)}$ and $y \in X_\varepsilon^{(j)}$, the triangle inequality gives

$$\left|d_\phi(x,y) - d_\phi(x_i^*,x_j^*)\right| \le d_\phi(x,x_i^*) + d_\phi(y,x_j^*).$$

Taking infimum over x,y yields

$$\left|d_\phi(X_\varepsilon^{(i)},X_\varepsilon^{(j)}) - C_{ij}\right| \le \sup_{x\in X_\varepsilon^{(i)}} d_\phi(x,x_i^*) + \sup_{y\in X_\varepsilon^{(j)}} d_\phi(y,x_j^*),$$

which tends to 0 by Lemma 4.3. □

6. Canalization as Gromov–Hausdorff collapse

Lemma 6.1 (Intra-basin collapse) *For each i there exists $D_i > 0$ such that for all sufficiently small ε,*

$$\operatorname{diam}(X_\varepsilon^{(i)}, d_\phi) \le D_i\, \phi(\kappa_i \varepsilon)\, \sqrt{\varepsilon}.$$

Proof For $x,x' \in X_\varepsilon^{(i)}$ we estimate through the minimum: $d_\phi(x,x') \le d_\phi(x,x_i^*) + d_\phi(x_i^*,x')$. Taking the supremum over x,x' and applying Lemma 4.3 gives the claim. □

Theorem 6.2 (Canalization as GH collapse) *Let $d_{\mathscr{F}}$ be the metric on $\{1,\dots,k\}$ given by $d_{\mathscr{F}}(i,i) = 0$ and $d_{\mathscr{F}}(i,j) = C_{ij}$ for $i \ne j$. Then*

$$(X_\varepsilon, d_\phi) \xrightarrow{\text{GH}} (\{1,\dots,k\}, d_{\mathscr{F}}) \qquad (\varepsilon \downarrow 0).$$

Proof Fix $\delta > 0$. Choose ε small such that for all i,

$$\operatorname{diam}(X_\varepsilon^{(i)}, d_\phi) < \delta/6$$

by Lemma 6.1, and for all $i \ne j$,

$$\left|d_\phi(X_\varepsilon^{(i)},X_\varepsilon^{(j)}) - C_{ij}\right| < \delta/6$$

by Lemma 5.3.

Define a correspondence $\mathscr{R} \subset X_\varepsilon \times \{1,\dots,k\}$ by $(x,i) \in \mathscr{R}$ iff $x \in X_\varepsilon^{(i)}$.

If $(x,i),(y,j) \in \mathscr{R}$ and $i = j$ then $d_{\mathscr{F}}(i,j) = 0$ while $d_\phi(x,y) \le \operatorname{diam}(X_\varepsilon^{(i)}, d_\phi) < \delta/6$. If $i \ne j$, then

$$\left|d_\phi(x,y) - d_\phi(X_\varepsilon^{(i)},X_\varepsilon^{(j)})\right| \le \operatorname{diam}(X_\varepsilon^{(i)}, d_\phi) + \operatorname{diam}(X_\varepsilon^{(j)}, d_\phi) < \delta/3,$$

and so

$$\left|d_\phi(x,y) - d_{\mathscr{F}}(i,j)\right| < \delta/3 + \delta/6 = \delta/2.$$

Thus the distortion of $\mathscr{R}$ is $< \delta$, which implies $d_{\text{GH}}((X_\varepsilon,d_\phi),(\{1,\dots,k\},d_{\mathscr{F}})) < \delta/2$. □

7. Collapse rate

Near x_i^*,

$$s(x) = \tfrac{1}{2}(x-x_i^*)^\top H_i (x-x_i^*) + O(|x-x_i^*|^3),$$

where $H_i = \operatorname{Hess} s(x_i^*)$ is positive definite. Let $\lambda_{\min}$ be the smallest eigenvalue of H_i.

Lemma 6.1 yields the scaling

$$\operatorname{diam}(X_\varepsilon^{(i)}, d_\phi) \le C\,\phi(\kappa_i \varepsilon)\,\sqrt{\varepsilon/\lambda_{\min}} \qquad (\varepsilon \downarrow 0)$$

for a constant C depending on the local quadratic bounds.

If $\phi(s) = s^\alpha$ with $\alpha > 0$, then

$$\operatorname{diam}(X_\varepsilon^{(i)}, d_\phi) = O\big(\varepsilon^{\alpha+1/2}\big).$$

Remark 7.1 (What controls the rate) *The exponent $\alpha + \frac{1}{2}$ combines how quickly motion becomes inexpensive near $s = 0$ (encoded by ϕ) and how quickly the basin radius shrinks (encoded by the quadratic model of s). Constants depend on the local condition number Λ_i/λ_i from Lemma 4.1.*

The upper bound is in fact sharp. We now establish a matching lower bound.

Proposition 7.2 (Matching lower bound on diameter) *Under assumptions* (A1)–(A4)*, for each i there exists $c_i > 0$ such that for all sufficiently small ε,*

$$\operatorname{diam}(X_\varepsilon^{(i)}, d_\phi) \;\ge\; 2\int_0^{\sqrt{2\varepsilon/\Lambda_i}} \phi\big(\tfrac{\lambda_i}{2}u^2\big)\,\mathrm{d}u.$$

In particular, for $\phi(s) = s^\alpha$ with $\alpha > 0$,

$$\operatorname{diam}(X_\varepsilon^{(i)}, d_\phi) = \Theta\big(\varepsilon^{\alpha+1/2}\big) \qquad (\varepsilon \downarrow 0).$$

Proof Let e be any unit eigenvector of $H_i = \operatorname{Hess} s(x_i^*)$ and set $R = \sqrt{2\varepsilon/\Lambda_i}$, where Λ_i is the largest eigenvalue of H_i. Define $x_\pm = x_i^* \pm Re$. By the upper quadratic bound (Lemma 4.1),

$$s(x_\pm) \le \tfrac{\Lambda_i}{2}R^2 = \varepsilon,$$

so $x_\pm \in X_\varepsilon^{(i)}$ for ε small enough that $R < r_i$.

Projection argument. Write $\pi(y) = \langle y - x_i^*, e\rangle$ for the signed distance from x_i^* along e. For any piecewise C^1 curve γ from x_+ to x_- we have $|\gamma'| \ge |\pi'(\gamma)|$. Moreover, the lower quadratic bound gives $s(\gamma(t)) \ge \frac{\lambda_i}{2}|\gamma(t) - x_i^*|^2 \ge \frac{\lambda_i}{2}\pi(\gamma(t))^2$ inside $B(x_i^*, r_i)$, and $s \ge \frac{\lambda_i}{2}r_i^2 > 0$ outside. Since ϕ is increasing,

$$\int \phi(s(\gamma))\,|\gamma'|\,\mathrm{d}t \;\ge\; \int \phi\big(\tfrac{\lambda_i}{2}\pi(\gamma)^2\big)\,|\pi'(\gamma)|\,\mathrm{d}t.$$

The projected path $u(t) = \pi(\gamma(t))$ starts at R, ends at $-R$, and by the intermediate value theorem visits every value in $(-R, R)$. Hence

$$\int \phi\big(\tfrac{\lambda_i}{2}u^2\big)\,|\mathrm{d}u| \;\ge\; \int_{-R}^{R} \phi\big(\tfrac{\lambda_i}{2}u^2\big)\,\mathrm{d}u \;=\; 2\int_0^R \phi\big(\tfrac{\lambda_i}{2}u^2\big)\,\mathrm{d}u,$$

since the integrand is even and nonnegative (backtracking only increases the integral).

Power-law evaluation. For $\phi(s) = s^\alpha$, the integral evaluates to

$$2\int_0^R \left(\tfrac{\lambda_i}{2}\right)^\alpha u^{2\alpha}\,\mathrm{d}u = \frac{2(\lambda_i/2)^\alpha}{2\alpha+1} R^{2\alpha+1} = \frac{2(\lambda_i/2)^\alpha}{2\alpha+1}\left(\frac{2\varepsilon}{\Lambda_i}\right)^{\alpha+1/2},$$

which is $\Theta(\varepsilon^{\alpha+1/2})$. Combining with the upper bound from Lemma 6.1 gives $\operatorname{diam}(X_\varepsilon^{(i)}, d_\phi) = \Theta(\varepsilon^{\alpha+1/2})$. □

8. Generalization to Morse–Bott landscapes

In biological applications, a "cell type" is not a single expression state but a manifold of states sharing the same phenotypic identity. We therefore generalize the framework from isolated minima to compact attracting submanifolds.

Definition 8.1 (Morse–Bott landscape) *We say that $s : \mathbb{R}^n \to [0,\infty)$ is a* Morse–Bott landscape *if the following hold:*

(B1)The zero set $\{s = 0\}$ is a disjoint union $M_1 \sqcup \cdots \sqcup M_k$ of compact connected smooth submanifolds of $\mathbb{R}^n$ (each without boundary).

(B2)At every $p \in M_i$ the normal Hessian

$$H_p^\perp := \operatorname{Hess} s(p)\big|_{(T_pM_i)^\perp}$$

is positive definite.

(B3)(Ridge separation) There exists $c > 0$ such that the connected components of $\{s < c\}$ containing distinct M_i have disjoint closures.

(B4)(Properness) $s(x) \to \infty$ as $|x| \to \infty$.

Condition (B2) is the standard Morse–Bott nondegeneracy: s is allowed to be constant (zero) along M_i but must grow quadratically in the normal directions. By compactness of each M_i, the normal eigenvalues are uniformly bounded: there exist $0 < \lambda_i^\perp \le \Lambda_i^\perp$ such that $\lambda_i^\perp |v|^2 \le \langle H_p^\perp v, v\rangle \le \Lambda_i^\perp |v|^2$ for all $p \in M_i$ and $v \in (T_pM_i)^\perp$.

Lemma 8.2 (Tubular quadratic control) *For each i there exists $\rho_i > 0$ such that for all x with $\operatorname{dist}(x, M_i) < \rho_i$,*

$$\tfrac{\lambda_i^\perp}{2}\operatorname{dist}(x,M_i)^2 \;\le\; s(x) \;\le\; \tfrac{\Lambda_i^\perp}{2}\operatorname{dist}(x,M_i)^2.$$

Proof In a tubular neighborhood of M_i, write $x = \exp_p(v)$ where $p = \pi_i(x)$ is the nearest-point projection onto M_i and $v \in (T_pM_i)^\perp$ with $|v| = \operatorname{dist}(x,M_i)$. Since $s|_{M_i} = 0$ and $\nabla s|_{M_i} = 0$ (because $M_i \subset \{s = 0\}$ with $s \ge 0$), the second-order Taylor expansion along the fiber gives $s(x) = \frac{1}{2}\langle H_p^\perp v, v\rangle + O(|v|^3)$. The uniform eigenvalue bounds and a compactness argument yield the claim for ρ_i small enough. □

Lemma 8.3 (Intra-component collapse in the Morse–Bott setting) *For each i there exists $D_i > 0$ such that for all sufficiently small ε,*

$$\operatorname{diam}(X_\varepsilon^{(i)}, d_\phi) \le D_i\, \phi(\kappa_i^\perp \varepsilon)\, \sqrt{\varepsilon},$$

where $\kappa_i^\perp = \Lambda_i^\perp / \lambda_i^\perp$ and $X_\varepsilon^{(i)}$ is the component of $\{s \le \varepsilon\}$ containing M_i. In particular, $\operatorname{diam}(X_\varepsilon^{(i)}, d_\phi) \to 0$.

Proof Fix $x, x' \in X_\varepsilon^{(i)}$. Let $p = \pi_i(x)$ and $p' = \pi_i(x')$ be their nearest points on M_i. Since M_i is connected, there exists a path $\sigma : [0,1] \to M_i$ from p to p'. Along σ, $s = 0$, so $\phi(s(\sigma)) = 0$ and the d_ϕ-length of σ is zero. Therefore

$$d_\phi(x,x') \le d_\phi(x,p) + d_\phi(p,p') + d_\phi(p',x') = d_\phi(x,p) + 0 + d_\phi(p',x').$$

For $d_\phi(x,p)$: parametrize the normal segment as $\gamma(t) = p + t(x-p)$ for $t \in [0,1]$. Since $|\gamma(t) - p| = t \operatorname{dist}(x, M_i)$, Lemma 8.2 gives $s(\gamma(t)) \le \frac{\Lambda_i^\perp}{2} t^2 \operatorname{dist}(x,M_i)^2 \le \frac{\Lambda_i^\perp}{\lambda_i^\perp} \varepsilon = \kappa_i^\perp \varepsilon$, where the second inequality uses $\operatorname{dist}(x,M_i)^2 \le 2\varepsilon/\lambda_i^\perp$ (from Lemma 8.2). Then $d_\phi(x,p) \le \phi(\kappa_i^\perp \varepsilon) \operatorname{dist}(x,M_i) \le \phi(\kappa_i^\perp \varepsilon) \sqrt{2\varepsilon/\lambda_i^\perp}$, exactly as in Lemma 4.3. The same bound applies to $d_\phi(p',x')$, giving the claim. □

The inter-basin analysis (Section 5) carries over verbatim: any path from M_i to M_j must cross the ridge $\{s \ge c\}$ and traverse the Euclidean gap, so $C_{ij} := d_\phi(M_i, M_j) > 0$.

Theorem 8.4 (Canalization for Morse–Bott landscapes) *Under* (B1)–(B4)*, with $d_{\mathscr{F}}(i,j) = C_{ij} = d_\phi(M_i, M_j)$,*

$$(X_\varepsilon, d_\phi) \xrightarrow{\text{GH}} (\{1,\dots,k\}, d_{\mathscr{F}}) \qquad (\varepsilon \downarrow 0).$$

Proof The proof is identical to that of Theorem 6.2: the correspondence $(x,i) \in \mathscr{R}$ iff $x \in X_\varepsilon^{(i)}$ has distortion tending to 0 by Lemmas 8.3 and the Morse–Bott analogue of Lemma 5.3. □

Remark 8.5 (Biological interpretation) *In the Morse–Bott picture, each cell type i is modelled by a manifold M_i of expression states—capturing the well-known fact that cells of the same type exhibit heterogeneous gene expression. Canalization now means that the entire manifold M_i, together with a tube of nearby states, collapses to a single point in the limit: the internal variability within a cell type is metrically negligible compared to the distance between types.*

9. Connection to Freidlin–Wentzell theory

We now connect the warped metric to the stochastic dynamics most commonly associated with Waddington's landscape: the overdamped Langevin equation

$$\mathrm{d}X_t = -\nabla s(X_t)\, \mathrm{d}t + \sqrt{2T}\, \mathrm{d}W_t, \tag{9.1}$$

where $T > 0$ is a noise intensity ("temperature") and W_t is standard Brownian motion in $\mathbb{R}^n$.

The quasi-potential as a warped length metric

In the Freidlin–Wentzell theory (Freidlin and Wentzell, 1998), the *quasi-potential* from a stable equilibrium a to a state b is

$$V(a,b) = \inf_{T>0} \inf_{\substack{\gamma\in C^1([0,T];\mathbb{R}^n)\\ \gamma(0)=a,\,\gamma(T)=b}} \frac{1}{2}\int_0^T \left|\dot\gamma(t) + \nabla s(\gamma(t))\right|^2 \mathrm{d}t.$$

For the gradient drift $b(x) = -\nabla s(x)$, the action functional simplifies to a reparametrization-invariant form. The following result is classical (see, e.g., (Freidlin and Wentzell, 1998, Ch. 4) and (Heymann and Vanden-Eijnden, 2008)); we include the short proof for the reader's convenience and to set notation.

Proposition 9.1 (Geometric action (Freidlin and Wentzell 1998; Heymann and Vanden-Eijnden 2008)) *For two global minima x_i^*, x_j^* with $s(x_i^*) = s(x_j^*) = 0$,*

$$V(x_i^*, x_j^*) \;=\; \inf_{\gamma} \int |\nabla s(\gamma)|\,|\mathrm{d}\gamma| \;=:\; d_{|\nabla s|}(x_i^*, x_j^*), \tag{9.2}$$

where the infimum is over piecewise C^1 paths connecting x_i^* to x_j^*.

Proof Expanding the action:

$$\frac{1}{2}\int_0^T |\dot\gamma + \nabla s(\gamma)|^2\,\mathrm{d}t = \frac{1}{2}\int_0^T |\dot\gamma|^2\,\mathrm{d}t + \int_0^T \langle \dot\gamma, \nabla s(\gamma)\rangle\,\mathrm{d}t + \frac{1}{2}\int_0^T |\nabla s(\gamma)|^2\,\mathrm{d}t.$$

The cross term equals $s(\gamma(T)) - s(\gamma(0)) = 0$ (since both endpoints have $s = 0$), so the action becomes $\frac{1}{2}\int|\dot\gamma|^2\,\mathrm{d}t + \frac{1}{2}\int|\nabla s(\gamma)|^2\,\mathrm{d}t$. By the AM–GM inequality, $\frac{1}{2}(|\dot\gamma|^2 + |\nabla s|^2) \geq |\dot\gamma|\,|\nabla s|$, with equality if and only if $|\dot\gamma(t)| = |\nabla s(\gamma(t))|$ for all t. The right-hand side $\int|\dot\gamma|\,|\nabla s(\gamma)|\,\mathrm{d}t = \int|\nabla s(\gamma)|\,|\mathrm{d}\gamma|$ is reparametrization-invariant, giving (9.2). Equality is achieved along *instantons*: paths satisfying $\dot\gamma = +\nabla s(\gamma)$ (time-reversed gradient flow) reparametrized to match the arclength condition. □

Remark 9.2 (Position-dependent vs. scalar weight) *The quasi-potential defines a warped length metric $d_{|\nabla s|}$ with* position-dependent *weight $\psi(x) = |\nabla s(x)|$, which in general is not a function of $s(x)$ alone. Our framework uses $\phi(s(x))$, a weight depending on x only through the scalar landscape value. The two frameworks coincide when level sets of s are round (all eigenvalues of* Hess *s equal); in general they are related as follows.*

Proposition 9.3 (Comparison near minima) *In the quadratic regime $|x - x_i^*| < r_i$, the gradient satisfies*

$$\frac{\sqrt{2}\,\lambda_i}{\sqrt{\Lambda_i}}\sqrt{s(x)} \;\leq\; |\nabla s(x)| \;\leq\; \frac{\sqrt{2}\,\Lambda_i}{\sqrt{\lambda_i}}\sqrt{s(x)}.$$

Consequently, for paths γ contained in $B(x_i^*, r_i)$,

$$\frac{\sqrt{2}\,\lambda_i}{\sqrt{\Lambda_i}}\,\ell_{\sqrt{s}}(\gamma) \;\leq\; \ell_{|\nabla s|}(\gamma) \;\leq\; \frac{\sqrt{2}\,\Lambda_i}{\sqrt{\lambda_i}}\,\ell_{\sqrt{s}}(\gamma), \tag{9.3}$$

where $\ell_w(\gamma) = \int w(\gamma)\,|\mathrm{d}\gamma|$ denotes the weighted length. When $\lambda_i = \Lambda_i$ (isotropic minimum) both constants equal $\sqrt{2\lambda_i}$.

Proof Write $h = x - x_i^*$ and $H_i = \operatorname{Hess} s(x_i^*)$. In the quadratic regime, $\nabla s(x) = H_i h + O(|h|^2)$ and $s(x) = \frac{1}{2} h^\top H_i h + O(|h|^3)$. The eigenvalue bounds on H_i give $\lambda_i |h| \le |H_i h| \le \Lambda_i |h|$ and $\frac{\lambda_i}{2}|h|^2 \le s(x) \le \frac{\Lambda_i}{2}|h|^2$. Therefore $|h| \le \sqrt{2s(x)/\lambda_i}$ and $|h| \ge \sqrt{2s(x)/\Lambda_i}$, so

$$|\nabla s(x)| \ge \lambda_i |h| \ge \lambda_i \sqrt{2s(x)/\Lambda_i} = \frac{\sqrt{2}\,\lambda_i}{\sqrt{\Lambda_i}} \sqrt{s(x)}$$

and

$$|\nabla s(x)| \le \Lambda_i |h| \le \Lambda_i \sqrt{2s(x)/\lambda_i} = \frac{\sqrt{2}\,\Lambda_i}{\sqrt{\lambda_i}} \sqrt{s(x)}.$$

Integrating along γ yields (9.3). □

Remark 9.4 (The dynamically natural choice $\alpha = \frac{1}{2}$) *Proposition 9.3 shows that near minima the quasi-potential weight $|\nabla s|$ is comparable to $\sqrt{s}$, which corresponds to $\phi(s) = s^{1/2}$ in our framework. The choice $\alpha = \frac{1}{2}$ therefore has a distinguished dynamical meaning: it is the unique power-law exponent for which the warped metric locally approximates the Freidlin–Wentzell quasi-potential. With this choice the collapse rate is* $\operatorname{diam} = \Theta(\varepsilon)$ *(linear in ε), and the inter-basin distances C_{ij} approximate the quasi-potential barriers controlling rare transitions between cell types.*

Explicit comparison in one dimension

For $n = 1$ with $s(x) = (x^2 - 1)^2$, the quasi-potential between the two minima is

$$V(-1,1) = \int_{-1}^{1} |s'(x)|\,\mathrm{d}x = \int_{-1}^{1} 4|x|(1-x^2)\,\mathrm{d}x = 2.$$

This is consistent with the classical formula for gradient systems: $V(x_i^*, x_j^*) = 2\,s(x_s)$ where x_s is the lowest saddle separating the two minima (Freidlin and Wentzell, 1998, Ch. 4). Here $s(0) = 1$ and $V = 2 \cdot 1 = 2$. The warped length distance with $\phi(s) = \sqrt{s}$ is

$$d_{\sqrt{s}}(-1,1) = \int_{-1}^{1} (1-x^2)\,\mathrm{d}x = \tfrac{4}{3}.$$

The ratio $V / d_{\sqrt{s}} = 3/2$ reflects the anisotropy of $|s'(x)|/\sqrt{s(x)} = 4|x|$, which ranges from 0 at the saddle to 4 at the minima.

10. Examples

10.1. *A one-dimensional double well*

Let $n = 1$ and $s(x) = (x^2 - 1)^2$, which has two nondegenerate global minima at $x^* = \pm 1$. Take $\phi(s) = s^\alpha$ with $\alpha > 0$. For ε small, X_ε is the union of two intervals around ± 1 and the limit metric space has two points.

In one dimension the minimizing curve between minima is the interval path, hence

$$C_{12} = d_\phi(-1,1) = \int_{-1}^{1} \phi(s(x))\,\mathrm{d}x = \int_{-1}^{1} (x^2-1)^{2\alpha}\,\mathrm{d}x < \infty.$$

By Proposition 7.2, $\operatorname{diam}(X_\varepsilon^{(i)}, d_\phi) = \Theta(\varepsilon^{\alpha+1/2})$. For the dynamically natural choice $\alpha = \frac{1}{2}$ (Remark 9.4), the collapse is linear: $\operatorname{diam} = \Theta(\varepsilon)$.

10.2. *A two-dimensional toggle switch*

A genetic toggle switch consists of two genes with mutual repression: when gene 1 is highly expressed, it suppresses gene 2, and vice versa (Gardner et al., 2000). This produces bistability with two stable cell fates. The standard ODE model uses Hill-function kinetics and is not a gradient system; its quasi-potential must be computed numerically (Wang et al., 2011). Here we use an explicit polynomial proxy that captures the essential bistable topology—two minima separated by a saddle—while remaining analytically tractable as a Morse function.

We model this via the landscape

$$s(x,y) = \big[(x-1)^2 + y^2\big]\big[x^2 + (y-1)^2\big], \tag{10.1}$$

on $\mathbb{R}^2$, where x and y represent the expression levels of genes 1 and 2 respectively.

Zero set and minima. The first factor vanishes only at $p_1 = (1,0)$ (gene 1 on, gene 2 off) and the second only at $p_2 = (0,1)$ (gene 2 on, gene 1 off), so $\{s = 0\} = \{p_1, p_2\}$.

Hessian computation. Write $s = fg$ with $f = (x-1)^2 + y^2$ and $g = x^2 + (y-1)^2$. At $p_1 = (1,0)$: $f = 0$, $g = 2$, $\nabla f = (0,0)$, so $\operatorname{Hess} s|_{p_1} = g(p_1) \cdot \operatorname{Hess} f|_{p_1} = 2 \cdot 2I = 4I$. By the symmetry $(x,y) \mapsto (y,x)$ that exchanges $p_1 \leftrightarrow p_2$, also $\operatorname{Hess} s|_{p_2} = 4I$. Both minima are isotropic with $\lambda_i = \Lambda_i = 4$ and condition number $\kappa_i = 1$.

Saddle point. The unique critical point in the interior region $\{f > 0, g > 0\}$ is the midpoint $p_s = (\frac{1}{2}, \frac{1}{2})$ (see the completeness check below); it has $s(p_s) = \frac{1}{4}$. The Hessian at p_s has eigenvalues ± 2, confirming a nondegenerate saddle. There are no other critical points (see below), so s is Morse with exactly two minima and one saddle.

Verification of (A1)–(A4). (A1) Morse: checked above. (A2) Two global minima at p_1, p_2 with $s = 0$. (A3) Ridge: for any $c < \frac{1}{4}$, the components of $\{s < c\}$ around p_1 and p_2 are separated by the saddle region. (A4) Properness: $s(x,y) \to \infty$ as $|(x,y)| \to \infty$ since s is a degree-4 polynomial with positive leading terms.

Completeness of critical-point analysis. Write $s = fg$ with $f = (x-1)^2 + y^2$ and $g = x^2 + (y-1)^2$, so $f, g \geq 0$ and

$$\nabla s = g\nabla f + f\nabla g.$$

If $f = 0$ then $(x,y) = (1,0) = p_1$, and if $g = 0$ then $(x,y) = (0,1) = p_2$. Otherwise $f, g > 0$ and the critical-point equations become

$$g(x-1) + fx = 0, \qquad gy + f(y-1) = 0.$$

Introduce centered coordinates $u = x - \frac{1}{2}$, $v = y - \frac{1}{2}$, set $r^2 = u^2 + v^2$, and note

$$f = r^2 + (v-u) + \tfrac{1}{2}, \qquad g = r^2 + (u-v) + \tfrac{1}{2}.$$

With $a := r^2 + \frac{1}{2}$ and $d := v - u$ (so $f = a + d$ and $g = a - d$), the two equations simplify to

$$2au + d = 0, \qquad 2av - d = 0.$$

Hence $v = -u$, and then $d = v - u = -2u$ together with $d = -2au$ gives either $u = 0$ (so $v = 0$ and $(x,y) = (\frac{1}{2}, \frac{1}{2}) = p_s$) or $a = 1$ (so $r^2 = \frac{1}{2}$ and $(u,v) = (\pm\frac{1}{2}, \mp\frac{1}{2})$, which correspond to p_1 and p_2). Therefore $\{p_1, p_2, p_s\}$ are all critical points of s.

Collapse rate. Since $\kappa_i = 1$ and $\lambda_i = 4$, Proposition 7.2 and Lemma 6.1 give

$$\operatorname{diam}(X_\varepsilon^{(i)}, d_\phi) = \Theta(\varepsilon^{\alpha+1/2}) \qquad (i = 1,2).$$

For $\alpha = \frac{1}{2}$: diam $= \Theta(\varepsilon)$.

Inter-basin distance. The straight-line path $\gamma(t) = (1-t,t)$, $t \in [0,1]$, connects p_1 to p_2 with $|\gamma'| = \sqrt{2}$ and

$$s(\gamma(t)) = 4t^2(1-t)^2.$$

This gives the upper bound

$$C_{12} \le \sqrt{2} \int_0^1 \phi(4t^2(1-t)^2)\,\mathrm{d}t.$$

For $\phi(s) = s^\alpha$:

$$C_{12} \le \sqrt{2} \cdot 4^\alpha \int_0^1 t^{2\alpha}(1-t)^{2\alpha}\,\mathrm{d}t = \sqrt{2} \cdot 4^\alpha B(2\alpha+1, 2\alpha+1),$$

where B is the Beta function. Some explicit values:

α	$1/2$	1	2
$C_{12} \le$	$\frac{\sqrt{2}}{3} \approx 0.471$	$\frac{2\sqrt{2}}{15} \approx 0.189$	$\frac{8\sqrt{2}}{315} \approx 0.036$

For a lower bound, any path from p_1 to p_2 must cross the ridge $\{s \ge c\}$ (for $c < \frac{1}{4}$) and traverse the Euclidean gap $w_{12} > 0$ between the basin closures. The general bound $C_{12} \ge \phi(c)\, w_{12}$ from Lemma 5.2 applies.

Biological interpretation. The landscape (10.1) models the two cell fates arising from mutual repression: state $p_1 = (1,0)$ is the "gene-1-dominant" fate and $p_2 = (0,1)$ is the "gene-2-dominant" fate. The warped metric makes each cell type metrically small (collapse rate $\Theta(\varepsilon^{\alpha+1/2})$) while preserving the inter-fate distance C_{12}. The ratio $C_{12}/\operatorname{diam}$ quantifies the *canalization strength*: larger values indicate more robust separation between fates. In the dynamically natural scaling $\alpha = \frac{1}{2}$, the inter-basin distance $C_{12} \approx 0.471$ should be compared with the Freidlin–Wentzell quasi-potential $V(p_1, p_2)$, which governs the rate of noise-induced fate switching.

11. Discussion and outlook

We have given a rigorous geometric formalization of canalization—the robustness of developmental outcomes—via Gromov–Hausdorff collapse of conformally warped sublevel sets. The main theorem (Theorem 6.2) and its Morse–Bott extension (Theorem 8.4) show that low sublevel sets of a landscape s collapse to a finite discrete space under the warped metric d_ϕ. The sharp collapse rate $\Theta(\varepsilon^{\alpha+1/2})$ (Proposition 7.2) quantifies how rapidly intra-basin distances vanish relative to inter-basin distances. The Freidlin–Wentzell connection (Propositions 9.1 and 9.3) anchors the choice $\alpha = \frac{1}{2}$ in stochastic dynamics.

Several natural extensions remain:

(E1) *Graph limits:* replacing X_ε by neighborhoods of the gradient-flow skeleton (minima, index-1 saddles, connecting orbits) may produce metric-graph GH limits, connecting to the Reeb graph and persistent homology.

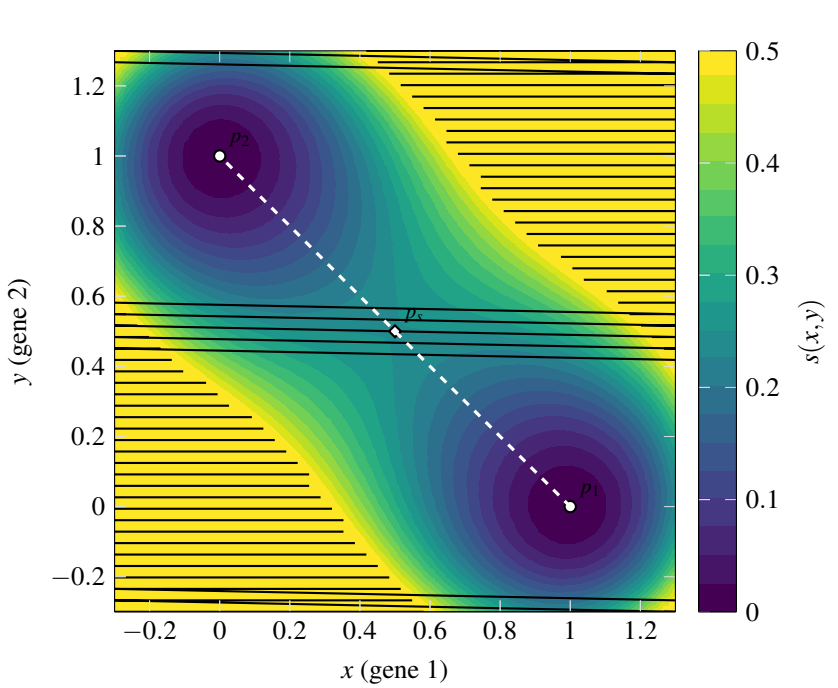

Figure 2. Contour plot of the toggle-switch landscape (10.1). The two minima $p_1 = (1,0)$ and $p_2 = (0,1)$ (circles) represent the two cell fates; the saddle $p_s = (\frac{1}{2}, \frac{1}{2})$ (diamond) separates the basins. The dashed line shows the straight-line path used to compute the upper bound on C_{12}. For small ε, the sublevel set $\{s \le \varepsilon\}$ consists of two small discs around p_1 and p_2 that collapse under d_ϕ.

(E2)*Curvature analysis:* the sectional curvature of g_ϕ diverges near $\{s = 0\}$; characterizing the blow-up rate and establishing Alexandrov curvature bounds $\kappa(\varepsilon)$ on the sublevel sets would place the paper in the RCD literature.

(E3)*Data-driven ϕ:* different near-zero behaviors of ϕ correspond to different canalization strengths. Given single-cell RNA-seq data and an inferred landscape $\hat{s}$, the warping function ϕ could in principle be estimated from observed variability scaling within basins.

(E4)*Non-gradient dynamics:* many gene-regulatory ODEs are not gradient systems. Extending the framework to quasi-potential landscapes defined via paths of minimum Freidlin–Wentzell action would cover this biologically important case.

(E5)*Wasserstein collapse:* placing the Boltzmann measure $\mu_T \propto e^{-s/T}$ on (X_ε, d_ϕ) and proving Wasserstein convergence to a discrete measure on the minima would connect to optimal transport.

Acknowledgements

The author thanks colleagues for discussions on geometric analysis and mathematical biology. The author also discloses the use of AI-assisted tools (Grok 4.2, Opus 4.6, and GPT-5.2) to help with drafting and editing text and with generating LaTeX/TikZ figure code; all mathematical claims, calculations, and final wording were reviewed and validated by the author. AI tools are not listed as authors.

REFERENCES

Bott, R. (1954) Nondegenerate critical manifolds. *Ann. of Math.* (2) 60, 248–261.

Burago, D., Burago, Y. and Ivanov, S. (2001) *A Course in Metric Geometry*. American Mathematical Society, Providence, RI.

Cheeger, J. and Gromov, M. (1986) Collapsing Riemannian manifolds while keeping their curvature bounded. I. *J. Differential Geom.* 23, 309–346.

Freidlin, M. I. and Wentzell, A. D. (1998) *Random Perturbations of Dynamical Systems*, 2nd edn. Springer, New York.

Fukaya, K. (1987) Collapsing of Riemannian manifolds and eigenvalues of Laplace operator. *Invent. Math.* 87, 517–547.

Gardner, T. S., Cantor, C. R. and Collins, J. J. (2000) Construction of a genetic toggle switch in *Escherichia coli*. *Nature* 403, 339–342.

Heymann, M. and Vanden-Eijnden, E. (2008) The geometric minimum action method: a least action principle on the space of curves. *Commun. Pure Appl. Math.* 61, 1052–1117.

Huang, S., Eichler, G., Bar-Yam, Y. and Ingber, D. E. (2005) Cell fates as high-dimensional attractor states of a complex gene regulatory network. *Phys. Rev. Lett.* 94, 128701.

Milnor, J. (1963) *Morse Theory*. Princeton University Press, Princeton, NJ.

Rizvi, A. H., Camara, P. G., Kandber, E. K. *et al*. (2017) Single-cell topological RNA-seq analysis reveals insights into cellular differentiation and development. *Nat. Biotechnol.* 35, 551–560.

Schiebinger, G., Shu, J., Tabaka, M. *et al*. (2019) Optimal-transport analysis of single-cell gene expression identifies developmental trajectories in reprogramming. *Cell* 176, 928–943.

Waddington, C. H. (1957) *The Strategy of the Genes*. Allen & Unwin, London.

Wang, J., Zhang, K., Xu, L. and Wang, E. (2011) Quantifying the Waddington landscape and biological paths for development and differentiation. *Proc. Natl. Acad. Sci. USA* 108, 8257–8262.

Zhou, J. X., Aliyu, M. D. S., Aurell, E. and Huang, S. (2012) Quasi-potential landscape in complex multi-stable systems. *J. R. Soc. Interface* 9, 3539–3553.